IEEE Open Journal of the Communications Society

Received XX Month, XXXX; revised XX Month, XXXX; accepted XX Month, XXXX; Date of publication XX Month, XXXX; date of current version 16 January, 2024.

Digital Object Identifier 10.1109/OJCOMS.2024.

Downlink Beamforming Strategies for Interference-Aware NGSO Satellite Systems

MAHDIS JALALI[1] *(Student Member, IEEE)*, EVA LAGUNAS[1] *(Senior Member, IEEE)*, ALIREZA HAQIQATNEJAD[2] *(Member, IEEE)*, STEVEN KISSELEFF[3] *(Senior Member, IEEE)*, SYMEON CHATZINOTAS[1] *(Fellow Member, IEEE)*

[1]Interdisciplinary Centre for Security Reliability and Trust (SnT), University of Luxembourg, Luxembourg
[2]OQ Technology, Leudelange, Luxembourg
[3]Fraunhofer Institute for Integrated Circuits IIS, Germany

CORRESPONDING AUTHOR: M. Jalali (e-mail: mahdis.jalali@uni.lu).

This work is financially supported by the Luxembourg National Research Fund (FNR) under the project MegaLEO (C20/IS/14767486).

ABSTRACT An important part of designing non-geostationary satellite orbit (NGSO) constellations is to ensure that they can co-exist with the legacy geostationary satellite orbit (GSO) systems in terms of interference levels. According to the current radio regulations defined by the International Telecommunication Union (ITU), NGSO systems shall not cause unacceptable interference to GSO systems. However, the traditional interference avoidance methods considered for the NGSO systems impact the coverage and overall service quality of their users. Embracing the trends of equipping NGSO satellites with phased array antennas, this paper investigates downlink beamforming strategies to improve NGSO users' service and mitigate the interference caused at GSO systems, ensuring seamless co-channel operation for NGSO and GSO network systems. Our proposed aggregate interference-constrained (AIC) beamforming optimization, limits the co-channel interference at GSO ground stations while minimizing the NGSO satellites' transmitted power. The AIC beamformer is designed under average channel state information (aCSI) to consider a practical scenario in NGSO satellite communications where acquiring perfect instantaneous channel information is challenging due to satellite mobility and long propagation roundtrip. Furthermore, for a more general scenario, this study considers robust AIC beamforming to account for the uncertainty in GSO ground stations' location when suppressing interference. Numerical results evidence the benefits of our proposed method ensuring service quality and providing the lowest probability for unaccepted interference levels at GSO ground stations among other benchmarks.

INDEX TERMS Beamforming, interference management, GSO-NGSO satellite co-existence.

I. INTRODUCTION

WE are witnessing the growth of non-geostationary satellite orbit (NGSO) mega-constellations driven by their promising potential to offer extensive and seamless global coverage [1]. This expanding deployment of mega-constellated satellite networks represents a significant shift in the satellite communication landscape, with several major players, including SpaceX, OneWeb, Telesat, and Amazon, actively working to establish global Internet networks [2], [3]. This transformative wave is characterized by innovation and significant investments, positioning low Earth orbit (LEO) satellites at the forefront of the evolving satellite communication domain [4].

The increasing adoption of NGSO satellites necessitates the prioritization of complex issues related to interference management and spectrum allocation. As more mega-constellations become operational, an increased number of satellites will share frequency bands, expanding coverage to more geographical regions and leading to greater overlap in satellite footprints. Consequently, the likelihood of interference is significantly rising [5]. This elevation in interference poses potential risks to existing geostationary satellite orbit

This work is licensed under a Creative Commons Attribution 4.0 License. For more information, see https://creativecommons.org/licenses/by/4.0/

(GSO) networks, which have priority of operation, increasing the likelihood of co-channel interference and interruptions in radio communication services [6], [7].

The NGSO-GSO spectrum challenge is currently a hot-topic in the International Telecommunication Union (ITU) Radio Regulations. Given the increasing proliferation of commercial NGSO systems, there is a new agenda item in the upcoming World Radiocommunication Conference's (WRC-27) aiming at the revision of the ITU regulations related to the interference levels caused by NGSO systems towards the GSO systems [8]. The international regulatory bodies are concerned about the space spectrum congestion and actively looking for strategies allowing an increased flexibility in spectrum access [9]. In this work, we focus on the satellite space-to-Earth transmission, where it is crucial to restrict the aggregation of emitted powers from satellites operating in the same frequency band toward the GSO ground stations [10].

Early works on NGSO-to-GSO downlink interference assumed that satellites lacked beamforming capabilities. This is due to the fact that early NGSO payload platforms did not incorporate advanced multi-antenna technology. In such cases, the proposed methodologies aimed at interference avoidance techniques employed at the NGSO satellites, to prevent the interference from occurring in the first place. Interference avoidance approaches include arc avoidance or exclusion zone [11], band-splitting [12], and look-aside methods [13]. While such techniques are effective in reducing interference at the GSO receivers, they have a strong negative impact on the coverage and quality-of-service (QoS) offered to the NGSO users, thus suggesting the need for more advanced solutions [7]. Even when considering power allocation alongside interference avoidance seems not enough to achieve a good coverage to the NGSO users, whose coverage gets impacted by the tilting of the NGSO satellites [14]. Moreover, the research in [15], concludes that the interference risks are a serious problem by presenting the probability of in-line events of OneWeb and Starlink LEO satellite constellations and a GSO receiver. To this reason, they suggest beam steering techniques to mitigate the NGSO-to-GSO interference.

While most of the earlier generation satellites were based on simple antenna architectures (e.g. single-feed per-beam), current antenna designs have evolved tremendously, embracing the progress and benefits observed in the terrestrial communication counterpart. Phased arrays are present in most of the recently manufactured satellites [16], opening the door to the use of beamforming. Beamforming[1] refers to the signal processing technique that enables steering the signal towards the desired direction using specific weight vectors, and reducing or eliminating mutual interference [17].

In the next section, we provide an review of the most relevant state of the art works related to interference management considering multi-antenna technology. Furthermore, we position our work with respect to general spectrum-sharing literature, and conclude by highlighting the main contributions of our work.

A. PREVIOUS WORKS AND CONTRIBUTIONS

1) PREVIOUS WORKS: GENERAL SPECTRUM SHARING

Dynamic spectrum access was initially proposed in early 2000's, providing the capability to unlicensed users to share the wireless channel with licensed users in an opportunistic manner [18]. Since then, the flexible and uncoordinated use of the spectrum has been investigated in many different scenarios and with different flavors. In this work, we face an interference-sharing scenario very relevant nowadays which is the NGSO-GSO spectrum co-existence, where the GSO system represents the "primary" system, and the NGSO constellation represents the "secondary" system.

The NGSO-GSO spectrum co-existence scenario poses some particularities, which are detailed in the following. First, the coverage area and transmit power levels of NGSO satellites differ significantly from those of secondary systems in cognitive terrestrial scenarios. NGSO constellations are composed of a dense network of small satellites flying in a coordinated manner. Such satellites provide coverage to areas with significant overlap. As a consequence, the aggregated interference becomes a concern. Moreover, considering the wide coverage of the satellites, a larger number of primary users (GSO ground stations) may fall within the NGSO satellite beams. Consequently, the interference issue between primary and secondary systems becomes more complex compared to terrestrial communications. Furthermore, the transmit power of the NGSO satellites is significantly higher compared to terrestrial systems due to the considerable propagation distances that their signals travel before reaching the Earth. In terrestrial cognitive literature, the secondary base station mostly considers low-range communications with reduced transmit power [19] and their aggregated impact is neglected due to spatial separation. In addition, most cognitive studies are based on the assumption of cooperation between primary and secondary, or on some sensing capabilities to avoid interference, or on the capabilities to acquire channel information on the primary user side [20]–[22]. These assumptions are not easily implemented in the NGSO-to-GSO interference problem, where the NGSO and GSO operators do not collaborate.

Our work focuses on in-orbit beamforming, and for that, we consider a uniform planar array (UPA) at each LEO satellites with a significant number of antenna elements. The array size in terms of number of elements for satellite is typically higher compared with that of the terrestrial domain [23]–[25] and this is justified by the spatial granularity requirements of the large-range propagation conditions of satellite systems. In general, the scale of our proposed scenario differs from the terrestrial cognitive networks. Moreover, the beamforming scenario in satellite communi-

[1]Throughout this paper, the terms "beamforming" and "precoding" are used interchangeably.

cation is particular due to the angular dimensions, where the directional beams exhibit significantly reduced angular separation owing to the high distance between the satellites and users. This is more pronounced when in our study we have considered a large number of LEO users and GSO ground stations. Many existing work in cognitive radio (e.g. [26]–[28]) considers the co-existence of a single primary system with one or two secondary systems. However, in practical space-based scenarios, several secondary satellites must co-exist alongside the primary system. Last but not least, most of the terrestrial cognitive radio literature considers the sum-rate maximization [29]–[31], or the fairness between competing secondary users [32], [33] as objective function. Instead, our work considers the optimization of the secondary system radio resource utilization (i.e. power) while satisfying the quality-of-service (QoS) of its users, and maintaining a limited level of interference to the GSO receivers.

In addition, considering the satellite-based cognitive systems, the existing research is mainly limited to overlay scenarios, beamhopping and database models [34], [35]. Works studying LEO as secondary system and GSO system as primary user are relatively scarce, predominantly focused on the beamhopping approach [36].

2) PREVIOUS WORKS: INTERFERENCE MANAGEMENT WITH BEAMFORMING

Despite extensive evaluation in terrestrial networks, the analysis of beamforming in satellite communication remains relatively limited. However, recent advancements in on-board multi-antenna technology have increased interest and exploration in this area [37]. In this section, we present some of the most relevant works and highlight the differences with our contributions.

The downlink beamforming for a massive multiple-input, multiple-output (MIMO) LEO satellite is performed by statistical channel state information in [38], where the beamformer is obtained to maximize the average signal-to-leakage-plus-noise ratio. In their subsequent work, [39], the authors expanded their research by incorporating UPA at the users' end. A double beamformer for the LEO satellite has been proposed in [40]. The first beamformer is to cluster users and the second employs zero-forcing (ZF) beamforming for users in the same cluster. Proposing beamforming for GSO satellites, the authors in [41] considered interference power constraints for the co-channel beams. Their proposed solution involves substituting the interference constraints with a harmonic-based mean, thus relaxing the optimization problem. However, all of the aforementioned studies focus on designing beamformers to mitigate inter-user and intra-system interference, whereas our approach additionally considers potential interference to the co-existing GSO systems. To our knowledge, the exploration of beamforming design for NGSO satellites aimed at mitigating co-channel interference to GSO systems has not been extensively addressed in the existing literature.

In our previous work, [42], we adopted beamforming for LEO satellites to prevent harmful interference. The ZF method was employed to derive the beamforming weights for steering toward LEO users and creating nulls at the Equator, where the interference potential on the GSO ground stations is more pronounced. It should be noted that the study considered an perfect channel state information (CSI) scenario, whereas the present work deviates from this simplification, accounting for more realistic scenarios by relaxing the assumption of perfect CSI.

The efficacy of MIMO beamforming relies on CSI which is challenging to obtain accurately in satellite communication mostly due to channel estimation uncertainty and aging [43]. To address this challenge, the use of average channel state information (aCSI) has been introduced for massive MIMO satellite communications [38], which we employ in this work. Furthermore, targeting interference mitigation at the GSO ground stations, the location information of these victim receivers impacts the effectiveness of beamforming methods. However, obtaining the precise positions of GSO ground stations is not straightforward as they do not belong to the LEO secondary system. Therefore, it is of importance to explore scenarios involving positioning errors and solutions to combat the resulting performance degradation. In the literature, studies have been done to evaluate and improve the performance of beamforming under channel uncertainty. A location-assisted beamforming is considered for an air platform in [44], where the performance of the beamformer under uncertainty of the angle of departure is evaluated. The work in [45] designs a beamformer for LEO satellite downlink transmission with CSI based on the angle of departure. A robust beamforming with deep learning methods is proposed for the angle deviations of users. However, these studies consider the channel uncertainty scenario for intra-system beamforming that accounts for uncertainty related to their own users. There are studies in cognitive radio systems where channel uncertainty in beamforming is considered. These studies mostly consider the uncertainty as an additive error to the channel coefficient, considering an ellipsoid uncertainty or Gaussian channel error [26], [28], [46]. Also, in non-cognitive studies, the independently and identically distributed (i.i.d.) complex Gaussian additive error is commonly considered for channel uncertainty modeling in robust beamforming studies, [47]–[49]. Despite the approach of directly added uncertainty error to the channel coefficients in these studies, an angle-based channel uncertainty model tailored to the satellite beamforming context remains the key to properly assess NGSO-to-GSO interference.

3) CONTRIBUTIONS OF THIS WORK

In this paper, we investigate the downlink beamforming for a LEO satellite constellation. We consider a UPA antenna

at LEO satellites for multiple-input, single-output (MISO) transmission, and mitigate the co-channel interference with GSO systems operating in the same frequency band. Inspired by the interference mitigation capability of beamforming methods [50], we exploit it for steering signals to targeted NGSO users and simultaneously controlling the interference towards the co-existing GSO systems. The efficacy of interference management with beamforming at the NGSO satellite is twofold in this study. Primarily, the beamforming will enable beam steering to the intended directions, reducing emissions to GSO systems. Secondly, we formulate our beamformer design problem to limit aggregate interference from LEO satellites to the GSO receiver side. Wherein, the aggregate interference is defined as the summed interference from the NGSO satellites' beams received at the GSO ground stations. As mentioned earlier, beamforming methods in the satellite-based literature are generally evaluated to increase the received signal power for the intended user and reduce inter-beam interference. Moreover, unlike the existing literature on satellite beamforming, here we consider the problem of multi-satellite beamforming and the resulting aggregate interference at the GSO system. Furthermore, given the crucial importance of power consumption in satellite systems, our problem formulation focuses on minimizing the total transmit power of the multiple LEO satellites. In addition, we consider the location uncertainty for our GSO interference mitigation constraint when obtaining the beamforming weights. We utilize the statistics of such uncertainty to develop a robust interference-limited beamforming method. To address the channel uncertainty challenge, we consider two characteristics: (i) the aCSI to model the imperfections on the channel gains, and (ii) the imperfect GSO ground location in terms of angular error.

Our major contributions in this work are summarized as follows:

- We design downlink beamforming for LEO satellite constellation to ensure service quality at LEO users and simultaneously limit interference at GSO ground stations. To the best of our knowledge, this is the first work to employ beamforming at the NGSO system for interference mitigation at the GSO ground stations' side. With this approach, we are able to serve the LEO users while using full-frequency reuse (FFR) for transmission and avoiding co-channel interference at the co-existing GSO systems. Inspired by the ITU aggregate interference limits, we consider the aggregate interference power from multiple LEO satellites to each GSO ground station and formulate it as the aggregate interference-constrained (AIC) to the beamforming problem.
- We formulate the beamforming optimization problem as a minimization of the overall transmit power while adhering to a minimum signal-to-interference-plus-noise ratio (SINR) for LEO users and a maximum aggregate interference-to-noise ratio (INR) at each GSO ground station. The problem is nonconvex and we consider the Lagrange duality relaxation of the problem to obtain the suboptimal solution.
- We compare our AIC beamforming method with the ZF technique and demonstrate the superior power reduction achieved by our approach.
- We study the uncertainty of GSO locations, to evaluate a more general and practical case. An angular inaccuracy of the channel steering vector is considered to model the uncertainty of GSO ground stations' locations. We formulate the problem for this positioning error and develop a robust AIC beamforming method.
- The formulated robust beamforming design is not convex and we apply the semi-definite relaxation (SDR) technique to transform the nonconvex problem into a convex semi-definite programming (SDP) form, which can be solved efficiently by existing interior methods. Through extensive numerical simulations, we demonstrate the efficiency of proposed techniques in suppressing interference for both accurate and uncertain GSO ground station locations.

B. ORGANIZATION AND NOTATIONS

The remainder of this paper is organized as follows. The system and channel model are described in Section II. In Sections III and IV, we present the problem formulation for two scenarios: certain and uncertain GSO ground station locations, respectively, followed by a detailed description of our proposed solutions. We provide the simulation results in Section V. Finally, Section VI concludes the paper.

The following notations are used throughout this paper. vectors and matrices are denoted by boldface small and capital letters, respectively. Notations, $(.)^H$, $(.)^T$, $|.|$ and $\|.\|_2$ denote Hermitian transpose, transpose, absolute, and ℓ_2-norm of matrix/vector, respectively. The operator $\otimes$ represents the Kronecker product, while $j = \sqrt{-1}$ denotes the imaginary unit. Additionally, $\mathbb{E}\{.\}$ indicates the expectation, and 'I' stands for the identity matrix. Moreover, $(\cdot)^+ = \max(x, \cdot)$, and $\lfloor . \rfloor$ represents the floor function symbol. Lastly, the curled inequality symbol $\succeq$ denotes a Hermitian positive semidefinite matrix.

II. SYSTEM AND CHANNEL MODEL

A. SYSTEM MODEL

We consider the downlink scenario for a mega-constellation with multi-beam LEO satellites equipped with phased array antennas. A GSO system operating in the same region using the same spectral band as the NGSO system is assumed. FFR is presumed to be implemented at each NGSO satellite where the proposed beamformer addresses the inter-beam interference concerns. In this study, to maximize the NGSO coverage, the Walker-star configuration has been assumed for the NGSO system. However, it is important to highlight that our proposed methodology extends beyond this particular satellite constellation configuration and holds its applicability

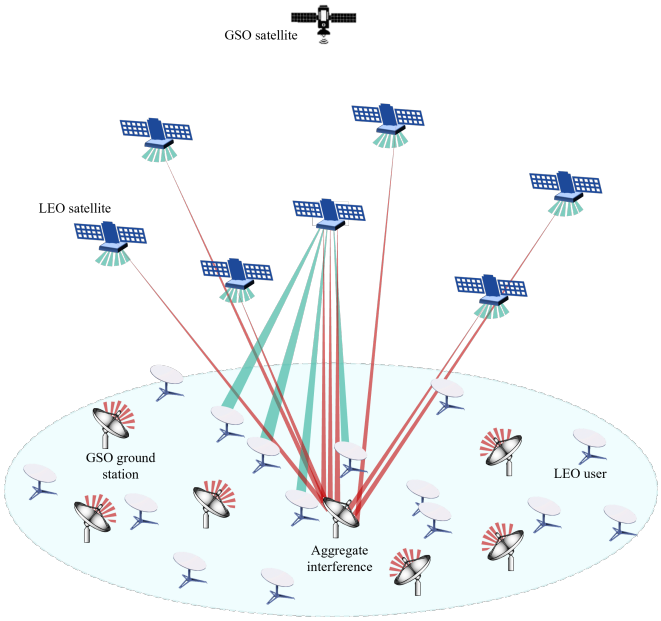

FIGURE 1. AIC beamforming for NGSO satellite system

across a broad spectrum of potential constellations. Fig. 1 illustrates the system model. The LEO multi-satellite beamformer design is carried out in a central approach at a ground controlling center. The system model consists of N LEO satellites, K users per satellite[1], and L GSO ground stations. We denote the LEO satellites with $i \in \{1, 2, 3, .., N\}$, and their users with $k \in \{1, 2, 3, .., K\}$. A single GSO satellite is assumed with $l \in \{1, 2, 3, .., L\}$ candidate ground station locations. These ground stations are considered to be critical stations whose location information is supposed to be known based on a database approach. This assumption is motivated by the databases of fixed service and broadcast satellite service available for some regions [51], [52]. As mentioned in [44], [52], At times, the databases may lack accuracy, and, for this reason, we consider the AIC beamforming problem under the uncertain location information of GSO ground stations.

B. CHANNEL MODEL

We assume the LEO satellites are equipped with UPA of M_x and M_y elements for the x- and y-axis, i.e. $M = M_x M_y$ antenna elements in total, and we note that $(K + L) \leq M$ is assumed. The array response vector of UPA is defined as [53],

$$\mathbf{v}\left(\theta^x, \theta^y\right) \triangleq \mathbf{v}^x\left(\theta^x, \theta^y\right) \otimes \mathbf{v}^y\left(\theta^x\right) \in \mathbb{C}^{M\times 1}, \tag{1}$$

where θ^x, θ^y denote the angles from x- and y-axis of the UPA. $\mathbf{v}^x$ and $\mathbf{v}^y$ present the x- and y-axis components of the array response vector. The vectors to the direction of (θ^x, θ^y) are given by,

$$\begin{aligned}\mathbf{v}^x\left(\theta^x, \theta^y\right) =& \frac{1}{\sqrt{M_x}}\Big[1, e^{-j(2\pi/\lambda)d_x \sin(\theta^y)\cos(\theta^x)}, \ldots, \\ & e^{-j(2\pi/\lambda)d_x(M_x-1)\sin(\theta^y)\cos(\theta^x)}\Big]^T \in \mathbb{C}^{M_x\times 1}, \\ \mathbf{v}^y\left(\theta^y\right) =& \frac{1}{\sqrt{M_y}}\Big[1, e^{-j(2\pi/\lambda)d_y \cos(\theta^y)}, \ldots, \\ & e^{-j(2\pi/\lambda)d_y(M_y-1)\cos(\theta^y)}\Big]^T \in \mathbb{C}^{M_y\times 1},\end{aligned} \tag{2}$$

where d_x and d_y are the array antenna spacing in x- and y-directions of the planar array. We assume similar element spacings in both directions, equivalent to half-wavelength.

The instantaneous downlink channel model for the i-th LEO satellite to its k-th user at time t and frequency, f follows [40],

$$\mathbf{h}_{i,k}(t, f) = q_{i,k}(t, f) \cdot e^{\left\{j2\pi\left[t\nu_{i,k}^{sat} - f\tau_{i,k}^{\min}\right]\right\}} \cdot \mathbf{v}_{i,k} \in \mathbb{C}^{M\times 1}, \tag{3}$$

where $\nu_{i,k}^{sat}$ is the Doppler shift of satellite and $\tau_{i,k}^{\min}$ denotes the minimum propagation delay in propagation paths. The array response vector for user k served by i-th satellite is represented by $\mathbf{v}_{i,k}$, calculated by (1). $q_{i,k}(t, f)$ is the complex channel gain and is defined as,

$$q_{i,k}(t, f) = \sum_{p=0}^{P_{i,k}-1} q_{i,k,p} \cdot e^{\left\{j2\pi\left[t\left(\nu_{i,k,p}-\nu_{i,k}^{sat}\right)-f\left(\tau_{i,k,p}-\tau_{i,k}^{\min}\right)\right]\right\}}, \tag{4}$$

where for k-th user of the i-th satellite, the number of propagation paths is denoted by $P_{i,k}$, the Doppler shift and propagation delay for p-th path are presented by $\nu_{i,k,p}$ and $\tau_{i,k,p}$, respectively. The complex-valued gain for the p-th path of the k-th user and i-th satellite is presented by $q_{i,k,p}$. The channel gain is the summation of the non-shadowed line-of-sight (LoS) path with $p = 0$, and $P_{i,k} - 1$ multipath components. In LEO satellite communication a Rician channel distribution is commonly considered which encompasses the LoS and non-LoS propagation paths [38]. As a result, we consider the channel gain $q_{i,k}(t, f)$ to have a Rician distribution with the Rician fading factor K_r, and power ${\eta_{i,k}^L}^2 = \mathbb{E}\{|q_{i,k}(t, f)|^2\} = (\lambda/4\pi r_{i,k})^2 (G_t^L)_{i,k}(G_r^L)_{i,k}$, where $(G_t^L)_{i,k}$, $(G_r^L)_{i,k}$, $r_{i,k}$, and λ denote the satellite transmit gain, user receiver gain, distance between the satellite and user, and the wavelength, respectively.

Considering delay and Doppler shift compensation, the received signal at the k-th user can be expressed as,

$$y_k = \mathbf{h}_{i,k}^H \mathbf{w}_{i,k} s_{i,k} + \mathbf{h}_{i,k}^H \sum_{j\neq k}^{K} \mathbf{w}_{i,j} s_{i,j} + n_k, \tag{5}$$

where $\mathbf{w}_{i,k} \in \mathbb{C}^{M\times 1}$ is the beamforming weight matrix for k-th user and i-th LEO satellite, and n_k presents the additive white Gaussian noise (AWGN) at the user. Thus, SINR of the k-th user served by the i-th LEO satellite can be obtained by,

[1]The user assignment in this work is done based on user-satellite shorter distance.

$$\mathrm{SINR}_{i,k} = \frac{|\mathbf{h}_{i,k}^H \mathbf{w}_{i,k}|^2}{\sum_{j\neq k}^{N} |\mathbf{h}_{i,k}^H \mathbf{w}_{i,j}|^2 + \sigma_k^2}, \tag{6}$$

where $\sigma_k^2 = K_b T_k^L B^L$, presents the user's noise power, K_b is the Boltzmann constant, T_k^L denotes equivalent noise temperature of the receiver, and B^L is the LEO bandwidth. It should be noted that based on simulations, the average interference power from GSO satellite signal to LEO users falls below the users' noise floor for the majority of instances. Thus, we neglect this interference in the users' SINR formulation.

Similarly, the channel model for the i-th LEO satellite to l-th GSO ground station can be derived as,

$$\mathbf{g}_{i,l}(t,f) = q_{i,l}^G(t,f) \cdot e^{\left\{j2\pi\left[t\nu_{i,l}^{sat} - f\tau_{i,l}^{\min}\right]\right\}} \cdot .v_{i,l}^G \in \mathbb{C}^{M\times 1}, \tag{7}$$

where $\mathbf{v}_{i,l}^G$ is the channel direction response vector from i-th LEO satellite to l-th GSO ground station obtained using (1) and (2). The channel gain is presented by $q_{i,l}^G(t,f)$, and follows the Rician distribution with factor K_r, and power ${\eta_{i,l}^G}^2 = \mathbb{E}\{|q_{i,l}^G(t,f)|^2\} = \left(\lambda/4\pi r_{i,l}^G\right)^2 (G_t^L)_{i,l}(G_r^G)_{i,l}$, where $(G_t^L)_{i,l}$, $(G_r^G)_{i,l}$, and $r_{i,l}^G$ denote the LEO satellite transmit gain, GSO ground station receiver gain, and distance between i-th LEO satellite to l-th GSO ground station, respectively.

In this way, the signal received at l-th GSO ground station in the co-existing scenario with LEO system, can be written as,

$$y_l = z_l\sqrt{p^G}x_l + \sum_{i}^{N} \mathbf{g}_{i,l}^H \left[\sum_{k}^{K} \mathbf{w}_{i,k}s_{i,k} + n_l\right] \tag{8}$$

where z_l is the channel from the GSO satellite to the l-th GSO ground station, p^G denotes the power transmission of GSO satellite, and n_l represents the noise at the GSO ground station. x_l and $s_{i,k}$ are the transmitted signals with zero mean and unit variance from GSO and LEO satellites, respectively. The second term in (8) is the interference signal from co-existing LEO satellites.

The aggregate interference from co-channel satellite beams at the l-th GSO ground station can be evaluated from INR as follows,

$$\mathrm{INR}_l = \frac{\sum_i^N \left[\sum_k^K |\mathbf{g}_{i,l}^H \mathbf{w}_{i,k}|^2\right]}{\sigma_l^2}, \tag{9}$$

where $\sigma_l^2 = K_b T_l^G B^G$ is the noise power at the receiver, where K_b, T_l^G, and B^G are the Boltzmann constant, equivalent noise temperature of the receiver and GSO bandwidth, respectively.

C. CSI ASSUMPTIONS

The SINR and INR equations presented in (6) and (9) rely on the instantaneous CSI (iCSI). However, as explained before, obtaining the iCSI for the LEO satellite communication is not straightforward. Considering the LEO channel model presented in (4), the magnitude of the channel gain is related to the carrier frequency, slant range, antenna gains, and multipath properties. The motion of the LEO satellite would affect the Doppler shift, propagation delay, and the response vector of the UPA. The Doppler and delay are considered to be compensated, while the channel gain is typically estimated using multiple pilot-based signals and averaging out the result. Moreover, in our scenario, the LEO users and GSO ground stations are assumed to be stationary, hence the angle-based part of the channel, i.e. the response vector is constant for the time block. Given these facts, it is reasonable to consider the LoS component dominates the propagation paths and is the primary link from the LEO satellite to the user, with propagation characteristics remaining relatively stable within a specific bandwidth [54] for the given transmission time slot. Thus, we utilize the aCSI derived from the Rician distribution statistical properties. Now, we employ the aCSI to address our beamforming problem and examine the average signal-to-interference-plus-noise (ASINR). This metric is defined as follows [38], [55],

$$\begin{aligned}\mathrm{ASINR}_{i,k} &= \frac{\mathbb{E}\left\{|\mathbf{h}_{i,k}^H \mathbf{w}_{i,k}|^2\right\}}{\mathbb{E}\left\{\sum_{j\neq k}^K |\mathbf{h}_{i,k}^H \mathbf{w}_{i,j}|^2 + \sigma_k^2\right\}} \\ &= \frac{{\eta_{i,k}^L}^2 |\mathbf{v}_{i,k}^H \mathbf{w}_{i,k}|^2}{\sum_{j\neq k}^K {\eta_{i,j}^L}^2 |\mathbf{v}_{i,k}^H \mathbf{w}_{i,j}|^2 + \sigma_k^2}.\end{aligned} \tag{10}$$

where the expectation is taken over the channels and $\mathbb{E}\{|\mathbf{h}_{i,k}^H \mathbf{w}_{i,k}|^2\} = \mathbb{E}\{|q_{i,k}|^2\}|\mathbf{v}_{i,k}^H \mathbf{w}_{i,k}|^2$ is considered. This equality holds due to no angle information error for the array response vectors, $\mathbf{v}_{i,k}$ and the resulting deterministic vector, $\mathbf{v}_{i,k}^H \mathbf{w}_{i,k}$.

Accordingly, we can define the average interference-to-noise ratio (ASINR) by taking the expectation over the channels and with the same assumptions obtain,

$$\begin{aligned}\mathrm{AINR}_l &= \frac{\mathbb{E}\left\{\sum_i^N \left[\sum_k^K |\mathbf{g}_{i,l}^H \mathbf{w}_{i,k}|^2\right]\right\}}{\mathbb{E}\{\sigma_l^2\}} \\ &= \frac{\sum_i^N \left[\sum_k^K {\eta_{i,l}^G}^2 |\mathbf{v}_{i,l}^{G\,H} \mathbf{w}_{i,k}|^2\right]}{\sigma_l^2}.\end{aligned} \tag{11}$$

We can see from the above equations for ASINR and AINR, that instead of instant channel values, the average gain of channels and the direction vectors are used to reduce the complexity of the iCSI obtaining process. In the following section, for the sake of conciseness, we will use the SINR and INR equations for the problem derivation and solution. Moreover, for the simulation results in Section V include both evaluations using the instantaneous CSI and aCSI where, aCSI refers to ASINR and AINR equations, while the mention of CSI entails SINR and INR equations.

This article has been accepted for publication in IEEE Open Journal of the Communications Society. This is the author's version which has not been fully edited and content may change prior to final publication. Citation information: DOI 10.1109/OJCOMS.2024.3406530

III. PROBLEM FORMULATION

Our objective is a LEO downlink beamforming design to achieve interference mitigation within the co-existing GSO system, while simultaneously ensuring that NGSO users receive a specified level of quality of service. To address this objective, we formulate the following problem,

$$\begin{aligned} \min_{\mathbf{w}_{i,k}} & \sum_{i}^{N}\sum_{k}^{K}\|\mathbf{w}_{i,k}\|_2^2 \\ \text{s.t. } & \text{SINR}_{i,k} \geq \gamma_k, \quad \forall i, \forall k, \\ & \text{INR}_l \leq \zeta_l, \quad \forall l, \end{aligned} \tag{12}$$

where γ_k refers to the SINR threshold for the k-th user of LEO satellite system, and ζ_l denotes the interference threshold for l-th GSO ground stations. The design problem in (12) aims to optimize the beamforming coefficients $\mathbf{w}_{i,k}$, corresponding to the i-th LEO satellite and the k-th LEO user, in order to minimize the total transmit power for the LEO satellites. The first constraint ensures a minimum SINR level for the k-th LEO user associated with the i-th LEO satellite, while the second constraint, AIC, establishes a limit on the aggregate INR at each GSO ground station. Clearly, a strict INR threshold may lead to infeasible problems whenever the LEO user and GSO ground station are too closely located. In this paper, we will assume feasibility holds as such problems can be solved with appropriate user-to-satellite assignment.

It should be noted that we have presented the problem and the subsequent equations assuming the availability of iCSI for brevity. However, the problem can be easily transformed for the aCSI case by considering ASINR and AINR equations from (10) and (11), as the constraints. In both cases, the channel is represented by a deterministic constant, either an instantaneous or average value.

The beamforming optimization problem in (12) is non-convex due to the first constraint, which has an indefinite quadratic form. In the following subsection, we show how to solve the problem with the Karush-Kuhn-Tucker (KKT) optimality conditions.

A. KKT OPTIMALITY CONDITIONS

In this section, we focus on deriving the closed-form of the optimal solution for the problem at hand. The derivation of this is facilitated through the application of Lagrangian theory. Despite the nonconvex nature of our proposed problem, the concept of strong duality remains applicable [50], [56].

The Lagrangian function of the problem is expressed as,

$$\begin{aligned} \mathcal{L}(\mathbf{w},\lambda,\alpha) = & \sum_i\sum_k \|\mathbf{w}_{i,k}\|_2^2 \\ & + \sum_i\sum_k \lambda_{i,k}\left(\sum_{j\neq k}^{K}\frac{1}{\sigma_k^2}|\mathbf{h}_{i,k}^H\mathbf{w}_{i,j}|^2 + 1 - \frac{|\mathbf{h}_{i,k}^H\mathbf{w}_{i,k}|^2}{\gamma_k\sigma_k^2}\right) \\ & + \sum_l \alpha_l\left(\frac{1}{\zeta_l\sigma_l^2}\sum_i\sum_k|\mathbf{g}_{i,l}^H\mathbf{w}_{i,k}|^2\right), \end{aligned} \tag{13}$$

where $\lambda_{i,k}$ and α_l are Lagrangian multipliers for the SINR and INR constraints, respectively.

Next, we take the derivative of the Lagrangian function for the KKT condition and set $\partial\mathcal{L}/\partial\mathbf{w}_{i,k} = 0$, as,

$$\begin{aligned} \partial\mathcal{L}/\partial\mathbf{w}_{i,k} = & \mathbf{w}_{i,k} + \sum_{j\neq k}^{K}\frac{1}{\sigma_k^2}\lambda_{i,j}\mathbf{h}_{i,j}\mathbf{h}_{i,j}^H\mathbf{w}_{i,k} \\ & - \frac{1}{\gamma_k\sigma_k^2}\lambda_{i,k}\mathbf{h}_{i,k}h_{i,k}^H\mathbf{w}_{i,k} \\ & + \sum_l\frac{\alpha_l}{\zeta_l\sigma_l^2}\mathbf{g}_{i,l}\mathbf{g}_{i,l}^H\mathbf{w}_{i,k} = 0. \end{aligned} \tag{14}$$

From this, we can derive a fixed-point equation for finding $\lambda_{i,k}$, as,

$$\begin{aligned} \lambda_{i,k}^{-1} = & \frac{1}{\sigma_k^2}(1+\frac{1}{\gamma_{i,k}}) \\ & \mathbf{h}_{i,k}^H\left(I + \sum_k\frac{\lambda_{i,k}}{\sigma_k^2}\mathbf{h}_{i,k}\mathbf{h}_{i,k}^H + \sum_l\frac{\alpha_l\mathbf{g}_{i,l}\mathbf{g}_{i,l}^H}{\zeta_l\sigma_l^2}\right)^{-1}\mathbf{h}_{i,k}, \end{aligned} \tag{15}$$

where $\lambda_{i,k}$ also appears on the right side of the equation and can be solved iteratively. Further, We can derive the following equation for optimal beamforming weights from (14), as,

$$\begin{aligned} \mathbf{w}_{i,k} = & \left(I + \sum_k\frac{\lambda_{i,k}}{\sigma_k^2}\mathbf{h}_{i,k}\mathbf{h}_{i,k}^H + \sum_l\frac{\alpha_l}{\zeta_l\sigma_l^2}\mathbf{g}_{i,l}\mathbf{g}_{i,l}^H\right)^{-1}\mathbf{h}_{i,k} \\ & \times\frac{\lambda_{i,k}}{\sigma_k^2}(1+\frac{1}{\gamma_k})\mathbf{h}_{i,k}^H\mathbf{w}_{i,k}. \end{aligned} \tag{16}$$

By the above equation, we can present a structure for the optimal weights as $\mathbf{w}_{i,k}^* = \sqrt{\mathbf{u}_{i,k}}\hat{\mathbf{w}}_{i,k}$, where $\mathbf{u}_{i,k}$ presents the power of beamforming and for the beamformer direction we have $\hat{\mathbf{w}}_{i,k}$ as,

$$\hat{\mathbf{w}}_{i,k} = \frac{\left(I + \sum_k\frac{\lambda_{i,k}}{\sigma_k^2}\mathbf{h}_{i,k}\mathbf{h}_{i,k}^H + \sum_l\frac{\alpha_l\mathbf{g}_{i,l}\mathbf{g}_{i,l}^H}{\zeta_l\sigma_l^2}\right)^{-1}\mathbf{h}_{i,k}}{\left\|\left(I + \sum_k\frac{\lambda_{i,k}}{\sigma_k^2}\mathbf{h}_{i,k}\mathbf{h}_{i,k}^H + \sum_l\frac{\alpha_l\mathbf{g}_{i,l}\mathbf{g}_{i,l}^H}{\zeta_l\sigma_l^2}\right)^{-1}\mathbf{h}_{i,k}\right\|}. \tag{17}$$

Next, we consider the complementary slackness condition for the SINR constraint where $\lambda_{i,k} > 0$ and the equality

holds for the SINR constraint at the optimal beamforming weights, resulting,

$$\begin{aligned} &\frac{\mathbf{u}_{i,k}|\mathbf{h}_{i,k}^H\hat{\mathbf{w}}_{i,k}|^2}{\gamma_k} - \sum_{j\neq k}^{K}\mathbf{u}_{i,j}|\mathbf{h}_{i,k}^H\hat{\mathbf{w}}_{i,j}|^2 = \sigma_k^2 \\ &\mathbf{u}_i\mathbf{M}_i = \sigma_k^2 \\ &[\mathbf{M}_i]_{m,n} = \begin{cases} \frac{1}{\gamma_{i,m}}|\mathbf{h}_{i,m}^H\hat{\mathbf{w}}_{i,m}|^2, & m=n \\ -|\mathbf{h}_{i,m}^H\hat{\mathbf{w}}_{i,n}|^2, & m\neq n, \end{cases} \end{aligned} \tag{18}$$

where $\mathbf{u}_i = [\mathbf{u}_{i,1}, .., \mathbf{u}_{i,k}, ..., \mathbf{u}_{i,K}]$ is the vector of beamforming powers of satellites and $[\mathbf{M}_i]_{m,n}$ denotes (m,n)th elements of the $\mathbf{M}_i$ matrix. Accordingly, we can find the optimal beamforming power as,

$$\mathbf{u}_i = (\mathbf{M}_i)^{-1}\sigma_k^2. \tag{19}$$

Now, we have the optimal beamforming as a function of Lagrangian multipliers. We can obtain the α_l multiplier through gradient descent as,

$$\alpha_l^{t+1} = \left(\alpha_l^t - \epsilon\left(\zeta_l - \tfrac{1}{\sigma_l^2}\textstyle\sum_i\sum_k|\mathbf{g}_{i,l}^H\mathbf{w}_{i,k}|^2\right)\right)^+, \tag{20}$$

where, t denotes the iteration number and ϵ is a small step size.

As a result, the steps to obtain the optimal beamforming weights are summarized in the Algorithm 1, where e is a small value that determines the stopping criterion of the iterative algorithm. In section V, the value of $e = 10^{-6}$ has been considered. Furthermore, following [57], the computational complexity order of this algorithm can be approximated by considering the complexity domination of the matrix inversion operations. The resulting complexity order is $\mathcal{O}(L_{itr}(4KNM^3 + 2NK^3))$ where L_{itr} presents the number of iterations required for the algorithm.

Algorithm 1 Proposed AIC beamforming optimization

Input: System parameters and thresholds.
Output: Optimal beamforming weights, $\mathbf{w}_{i,k}^*$

1: Initialize Lagrangian variables, $\lambda_{i,k} > 0, \alpha_l > 0$
2: **while** $\frac{\sum_i\sum_k|\mathbf{g}_{i,l}^H\mathbf{w}_{i,k}|^2}{\sigma_l^2} - \zeta_l > e$:
3: Find $\lambda_{i,k}$ from equation (15) with fixed point method,
4: Calculate beamforming weight directions from (17),
5: Calculate beamforming weight powers from (19) and obtain beamforming weights,
6: Update α_l variables using (20),
7: **end while**
8: **return** $\mathbf{w}_{i,k}^*$

IV. GSO GROUND STATION LOCATION UNCERTAINTY

As previously discussed, the aCSI shall be considered for practical designs of MISO downlink LEO beamforming. This will allow us to use channel power statistics and position information for users and restricted GSO ground station locations when designing the beamformer weights. The effectiveness of this assumption will be shown in Section V when comparing the performance of both iCSI and aCSI. In addition, the inter-system interference avoidance from LEO satellites to GSO ground stations depends on the accuracy of the GSO ground station location information for determining the nulling direction. As mentioned in section II, the inconsistencies in the databases' accuracy, prompt our consideration of the AIC beamforming problem under uncertain location information and positioning errors.

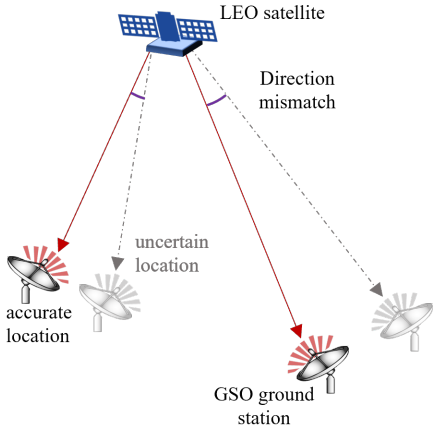

FIGURE 2. **Uncertainty in beamforming model**

In this section, inspired by the notation in [45], we add the uncertainty of the restricted directions. We assume that the estimation of the GSO ground station location is imperfect, i.e. it contains angular errors as depicted in Fig. 2. In this scenario, The accurate location angles are represented as follows,

$$\theta^x = \hat{\theta^x} + \delta_{uc}^x, \qquad \theta^y = \hat{\theta^y} + \delta_{uc}^y. \tag{21}$$

where the actual angles, θ^x, θ^y are a summation of the estimated angles, $\hat{\theta^x}$, $\hat{\theta^y}$ and the estimation error angles denoted by δ_{uc}^x, δ_{uc}^y. Now for $\mathbb{E}\{\mathbf{g}_{i,l}\mathbf{g}_{i,l}^H\}$, we have,

$$\mathbb{E}\{\mathbf{g}_{i,l}\mathbf{g}_{i,l}^H\} = |q_{i,l}|^2\mathbb{E}\{\mathbf{v}_{i,l}^G(\mathbf{v}_{i,l}^G)^H\} \tag{22}$$

The expectation is calculated based on the probability distribution of the angles' errors. For the location uncertainty, we assume a bounded uncertainty region and consider a uniform distribution for δ_{uc}^x and δ_{uc}^y as,

$$\delta_{uc}^x \sim \text{Uniform}(a_x, b_x), \quad \delta_{uc}^y \sim \text{Uniform}(a_y, b_y), \tag{23}$$

where a_x , a_y denote the lower boundaries, and b_x , b_y present the upper boundaries for the uniform distributions. The expectation, $\mathbb{E}\{\mathbf{v}_{i,l}^G(\mathbf{v}_{i,l}^G)^H\}$ is rewritten applying equation (1) and Kronecker product property as,

$$\mathbb{E}\{\mathbf{v}_{i,l}^G(\mathbf{v}_{i,l}^G)^H\} = \mathbb{E}\{(\mathbf{v}_{i,l}^G)^x((\mathbf{v}_{i,l}^G)^x)^H \otimes (\mathbf{v}_{i,l}^G)^y((\mathbf{v}_{i,l}^G)^y)^H\}. \tag{24}$$

The m,n-th element of the expectation matrix is calculated as,

$$\begin{aligned}\mathbb{E}\{[\mathbf{v}_{i,l}^G(\mathbf{v}_{i,l}^G)^H]_{m,n}\} &= \frac{1}{M}\frac{1}{(b_x-a_x)(b_y-a_y)}\\ &\times\int_{a_x}^{b_x}\int_{a_y}^{b_y}\exp(-j\pi\{\vartheta_{i,l}^x(\alpha-\beta)\\ &-\vartheta_{i,l}^y(n-m+M_y(\alpha-\beta))\})\,d\delta_{uc}^x d\delta_{uc}^y\end{aligned} \tag{25}$$

where

$$\begin{aligned}&\vartheta_{i,l}^x = \sin\left(\hat{\theta^y}+\delta_{uc}^y\right)\cos\left(\hat{\theta^x}+\delta_{uc}^x\right),\\ &\vartheta_{i,l}^y = \cos\left(\hat{\theta^y}+\delta_{uc}^y\right),\\ &\alpha=\lfloor m/M_y\rfloor,\quad \beta=\lfloor n/M_y\rfloor,\\ &m=n=[0,...,M-1].\end{aligned}$$

By solving the integral we have the following result for the expectation matrix elements,

$$\begin{aligned}&\mathbb{E}\left\{[\mathbf{v}_{i,l}^G(\mathbf{v}_{i,l}^G)^H]_{m,n}\right\}\\ &=\begin{cases}\frac{1}{M}, & n=m,\alpha=\beta;\\ \frac{1}{M}\frac{1}{\Delta_x}\frac{2e^{j\pi(n-m)\cos(\hat{\theta}_y)}\sin\left(\pi(n-m)\sin(\hat{\theta}_y)b_y\right)}{\pi(n-m)\sin(\hat{\theta}_y)}, & n\neq m,\alpha=\beta;\\ \frac{1}{M}\frac{4Z}{\Delta_x\Delta_y}\frac{\sin(Yb_x)\sin(\pi Xb_y)}{\pi XY}, & n\neq m,\alpha\neq\beta,\end{cases}\end{aligned} \tag{26}$$

where,

$$\begin{aligned}X &= (\alpha-\beta)\cos(\hat{\theta}_x)\cos(\hat{\theta}_y)\\ &\quad+(n-m+(\alpha-\beta)M_y)\sin(\hat{\theta}_y),\\ Y &= \pi(\alpha-\beta)\sin(\hat{\theta}_x)\sin(\hat{\theta}_y),\\ Z &= e^{j\pi(n-m+M_y(\alpha-\beta))\cos(\hat{\theta}_y)-j\pi(\alpha-\beta)\cos(\hat{\theta}_x)\sin(\hat{\theta}_y)},\\ \Delta_x &= b_x-a_x,\quad \Delta_y=b_y-a_y.\end{aligned}$$

The matrix $\mathbb{E}\{\mathbf{v}_{i,l}^G(\mathbf{v}_{i,l}^G)^H\}$ is obtained by derivation of its elements from the above formulation. Now we can obtain the expectation over the channel covariance matrix for the GSO ground stations by replacing the calculated matrix into (22). This leads us to reformulate our beamforming problem in (12) to account for the positioning errors related to the AIC, as,

$$\begin{aligned}&\min_{\mathbf{w}_{i,k}}\sum_i^N\sum_k^K\|\mathbf{w}_{i,k}\|_2^2\\ &\text{s.t.}\ \frac{|q_{i,k}|^2\mathbb{E}\left\{|\mathbf{v}_{i,k}^H\mathbf{w}_{i,k}|^2\right\}}{\sum_{j\neq k}^K|q_{i,j}|^2\mathbb{E}\left\{|\mathbf{v}_{i,k}^H\mathbf{w}_{i,j}|^2\right\}+\sigma_k^2}\geq\gamma_k,\forall i,\forall k,\\ &\frac{\sum_i^N\left[\sum_k^K|q_{i,l}^G|^2\mathbb{E}\left\{|\mathbf{v}_{i,l}^{G\,H}\mathbf{w}_{i,k}|^2\right\}\right]}{\sigma_l^2}\leq\zeta_l,\quad\forall l.\end{aligned} \tag{27}$$

We can equally rewrite the problem as follows,

$$\begin{aligned}&\min_{\mathbf{w}_{i,k}}\sum_i^N\sum_k^K\mathbf{w}_{i,k}\mathbf{w}_{i,k}^H\\ &\text{s.t.}\ \frac{|q_{i,k}|^2\mathbf{w}_{i,k}^HE\{\mathbf{v}_{i,k}\mathbf{v}_{i,k}^H\}\mathbf{w}_{i,k}}{\sum_{j\neq k}^K|q_{i,j}|^2\mathbf{w}_{i,j}^HE\{\mathbf{v}_{i,k}\mathbf{v}_{i,k}^H\}\mathbf{w}_{i,j}+\sigma_k^2}\geq\gamma_k,\forall i,\forall k,\\ &\frac{\sum_i^N\left[\sum_k^K|q_{i,l}^G|^2\mathbf{w}_{i,k}^HE\{\mathbf{v}_{i,l}^G\mathbf{v}_{i,l}^{G\,H}\}\mathbf{w}_{i,k}\right]}{\sigma_l^2}\leq\zeta_l,\quad\forall l,\end{aligned} \tag{28}$$

which is a nonconvex quadratically constrained quadratic program (QCQP) [58]. We define $\mathbf{W}_{i,k}=\mathbf{w}_{i,k}\mathbf{w}_{i,k}^H$, which adds the positive semidefinite (PSD) and ranke-one constraints to the problem. Furthermore, following the equality $\mathbf{w}^H\mathbf{R}\mathbf{w}=Tr\left(\mathbf{R}\mathbf{w}\mathbf{w}^H\right)=Tr\left(\mathbf{R}\mathbf{W}\right)$, we can reformulate the problem as follows,

$$\min_{\mathbf{W}_{i,k}}\sum_i Tr\left(\mathbf{W}_{i,k}\right) \tag{29a}$$

$$\begin{aligned}&\text{s.t.}\frac{1}{\gamma_k}Tr\left(\mathbf{R}_{i,k}^{ch}\mathbf{W}_{i,k}\right)\geq\\ &\qquad\sum_{j\neq k}^K Tr\left(\mathbf{R}_{i,k}^{ch}\mathbf{W}_{i,j}\right)+\frac{\sigma_k^2}{|q_{i,k}^G|^2},\end{aligned} \tag{29b}$$

$$\frac{1}{\sigma_l^2}\sum_i^N\sum_k^K|q_{i,l}^G|^2Tr\left(\mathbf{R}_{i,l}^{intf}\mathbf{W}_{i,k}\right)\leq\zeta_l,\quad\forall l \tag{29c}$$

$$\mathbf{W}_{i,k}\succeq 0, \tag{29d}$$

$$rank(\mathbf{W}_{i,k})=1. \tag{29e}$$

where $\mathbf{R}_{i,k}^{ch}=E\{\mathbf{v}_{i,k}\mathbf{v}_{i,k}^H\}$ and $\mathbf{R}_{i,l}^{intf}=E\{\mathbf{v}_{i,l}^G\mathbf{v}_{i,l}^{G\,H}\}$. The problem is still nonconvex due to the rank-one constraint. We can apply the SDR method [59], to transform the problem into a SDP. Accordingly, we remove the rank-one constraint and the approximated problem is rewritten as,

$$\begin{aligned}\min_{\mathbf{W}_{i,k}}\quad&\textstyle\sum_i Tr\left(\mathbf{W}_{i,k}\right)\\ \text{s.t.}\quad&(29b),(29c),(29d)\end{aligned} \tag{30}$$

The problem above is a convex SDP and can be solved optimally and efficiently with the interior-point method [58]. Following this, we determine the rank of the derived solution. If the solution proves to be rank-one, the optimal beamforming vector is obtained as $\mathbf{W}_{i,k}^*=\mathbf{w}_{i,k}^*\mathbf{w}_{i,k}^{*\,H}$. Otherwise, if the solution has the rank, $r\neq 1$, we employ a rank-one approximation via eigenvalue decomposition. Thus, the beamforming vector is obtained as, $\mathbf{w}_{i,k}^*=\sqrt{\lambda_1}\mathbf{q}_1$, where λ_1, and $\mathbf{q}_1$ are the largest eigenvalue and its corresponding eigenvector, respectively.

The algorithm for solving the beamforming problem with uncertainty is presented in Algorithm 2. The computational complexity of this algorithm is concentrated in the third step, which involves solving problem (30). According to [60], We can approximate the order of computation complexity as $\mathcal{O}(\sqrt{L+NK(1+M)}(KNM^2)^3)$.

Centralized approaches like the ones presented in this work are typically computationally intense. However, the centralized solution is the only one that can effectively manage the coupling interference constraint. Satellite operators mostly count with high performance infrastructure co-located with the control stations, which can host certain level of computation effort. Comparison with a pure decentralized algorithm is provided in Section V.

Algorithm 2 Proposed robust AIC beamforming optimization

Input: a_x, a_y, b_x, b_y

Output: $\mathbf{w}_{i,k}^*$

1: Calculate covariance matrix of LEO channels to each user, $\mathbf{R}_{i,k}^{ch}$,
2: Calculate the interference channel covariance matrix of LEO satellites to each GSO ground station, $\mathbf{R}_{i,l}^{intf}$, with equation (26),
3: Solve the beamforming problem from (30) and obtain $\mathbf{W}_{i,k}^*$,
4: **if** $\mathbf{W}_{i,k}^*$ is rank-one **then**
5: $\quad \mathbf{W}_{i,k}^* = \mathbf{w}_{i,k}^* \mathbf{w}_{i,k}^{*H}$,
6: **else**
7: $\quad$ obtain beamforming weights with eigenvalue decomposition, i.e., $\mathbf{w}_{i,k}^* = \sqrt{\lambda_1}\mathbf{q}_1$,
8: **end if**
9: **return** $\mathbf{w}_{i,k}^*$

V. SIMULATION RESULTS

In this section, we present the simulation results for our beamforming method. We select a sub-set of 7 neighboring LEO satellites that are extracted from a bigger constellation whose characteristics are presented in Table 1. LEO satellites are equipped with UPA antenna of size $M_x = M_y = 16$, and on the users' side we consider single antenna. The system parameters considered in the simulations are shown in Table 2. We also assume 20 GSO ground stations are randomly distributed. In our simulations, we adopt the ITU recommendation for the interference threshold level, as defined in [61]. This threshold is set such that it does not induce a violation exceeding 6% of the clear-sky satellite system noise, equivalent to an INR threshold of -12.2 dB. Furthermore, we assume that the SINR threshold and INR thresholds are the same for different users and GSO ground stations, hence, $\gamma_k = \gamma$ and $\zeta_l = \zeta$.

To provide an evaluation of our centralized beamforming approach, we first compare it with a distributed optimization model. In this distributed model, the beamforming is designed individually for each satellite, and the aggregated interference limit is managed by assuming that the contribution to the interference term caused by the NGSO satellites is uniformly distributed accross the number of satellites. This is a lower band for the interference of each separate satellite at the GSO ground station. Fig. 3 presents the total transmit power for each satellite comparing our method and the distributed approach, considering, $L = 15$, $K = 15$, $\gamma = 14$dB, and $\zeta = -12.2$. As expected, the results indicate higher power consumption in the distributed model due to the stricter interference threshold.

TABLE 1. LEO Constellation Parameters

Constellation configuration	Walker-star
Altitude	1200 km
Inclination angle	87.9°
Number of orbits	56
Satellites per orbit	56

TABLE 2. Simulation Parameters

Parameter	Value
Number of LEO satellites	7
Number of GSO ground stations	20
Frequency band	19.7GHz, [63]
Element spacing, $d_x = d_y$	$\lambda/2$, [38]
Rician channel factor, K_r	10 dB, [55]
Antenna elements on x- and y-axes	16×16, [38]
Bandwidth GSO ground station	500 MHz, [63]
Antenna diameter of GSO ground stations	0.7 m, [64]
Antenna pattern of GSO ground stations	[64]
Noise temperature	300 K
Antenna diameter of LEO users	0.3 m, [65]
Antenna pattern of LEO users	[65]
Longitude GSO satellite	25.6°
Latitude GSO satellite	0°

For comparison, we consider two other techniques: Zero Forcing (ZF) and Maximum Ratio Transmission (MRT) [62]. Table 3 provides a comparative evaluation of MRT method and our proposed AICBF approach for maintaining the INR level at the GSO ground stations. Results are obtained for $L = 20$, $K = 15$, $\gamma = 12$dB, and $\zeta = -12.2$, considering iCSI in this scenario. The outcomes reveal unsatisfactory performance with the MRT method. Exceeding interference thresholds are experienced during different realizations of users' distribution. This can be attributed to the inherent design of the MRT method, which maximizes signal-to-noise ratio (SNR) at the intended user without addressing inter-beam interference or any attempt to prevent interference to the GSO ground receivers. Meanwhile, the ZF beamformer consistently meets the constraints. Consequently, we exclusively rely on the ZF beamformer as a benchmark for our study.

In the following subsections, We present the results for both scenarios of certain and uncertain GSO location information.

A. GSO GROUND STATION LOCATION CERTAINTY RESULTS

First, we evaluate the performance of our proposed beamforming method while assuming the GSO ground station

This article has been accepted for publication in IEEE Open Journal of the Communications Society. This is the author's version which has not been fully edited and content may change prior to final publication. Citation information: DOI 10.1109/OJCOMS.2024.3406530

TABLE 3. Simulation Results for MRT Method

	INR compliance rate	Maximum INR
AICBF	100%	-12.2 dB
MRT	44.77%	19.07 dB

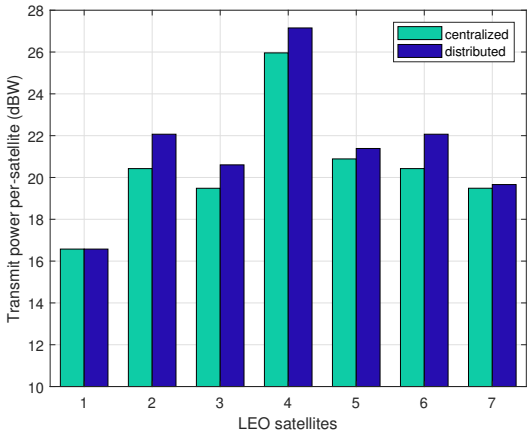

FIGURE 3. Transmit power for each satellite considering centralized and distributed beamforming design.

locations are known and fixed. To compare the results we consider four distinct cases alongside the ZF beamforming method as a benchmark. These methods are listed as,

- **iCSI-BF**: We assume we have iCSI for all channels and apply the beamforming method without considering the interference constraint. In this case, the beamforming is only designed to steer to LEO users without mitigating possible interference to GSO ground stations.
- **iCSI-AICBF**: For this case we assume iCSI and solve the beamforming problem as defined in the Algorithm 1. For this scenario, beamforming will be designed to both steer to LEO users and mitigate the interference at GSO ground stations.
- **aCSI-BF**: Considers aCSI and the ASINR constraint for the beamforming techniques. This is the same as iCSI-BF but considering aCSI instead of iCSI.
- **aCSI-AICBF**: This is our proposed method where we utilize the aCSI, ASINR and AINR to both steer to LEO users and mitigate the aggregate interference at GSO ground stations. This is the same as iCSI-AICBF but considering aCSI instead of iCSI.
- **iCSI-ZF**: The ZF beamforming is applied, considering iCSI. The resulting beamformer will nullify the interference at neighboring users as well as coexisting GSO ground stations.
- **aCSI-ZF**: This is the same as iCSI-ZF but considering aCSI instead of iCSI.

It should be noted that for all the above cases when computing the resulting SINR and INR at the receiver side, the actual channel coefficients are considered.

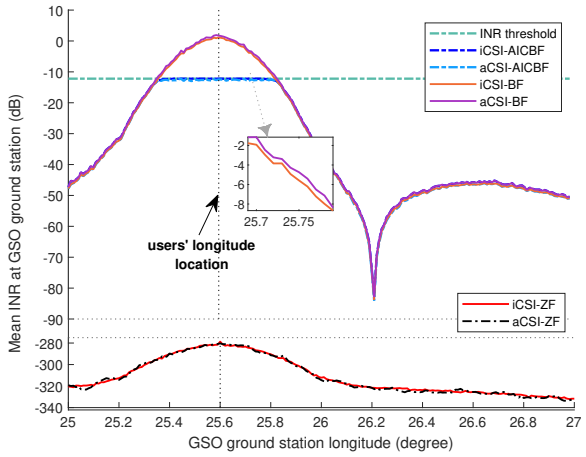

FIGURE 4. Mean INR level for the single LEO satellite and two users at (-0.2,25.6) and (0.2,25.6), over varying GSO ground station longitude locations considering $\zeta = -12.2$dB, $\gamma = 12$dB.

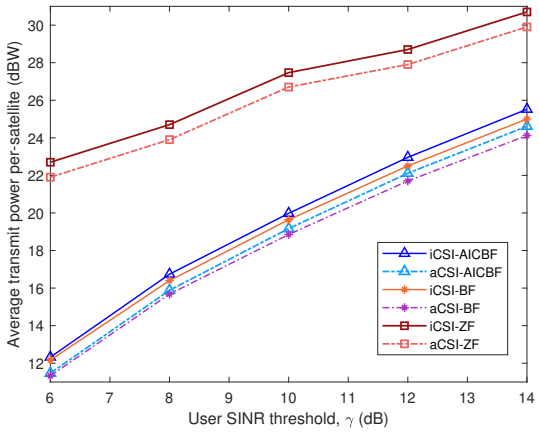

FIGURE 5. Mean satellite beamforming power for different SINR thresholds at LEO users considering $K = 15$, $\zeta = -12.2$dB.

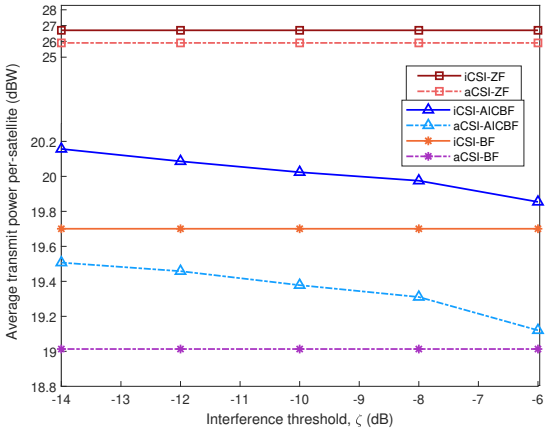

FIGURE 6. Mean satellite beamforming power for different interference thresholds at GSO ground stations considering $K = 15$, $\gamma = 10$dB.

The results are averaged for 400 iterations of random placement of LEO users. We begin by demonstrating the interference levels for a simple scenario with one LEO satellite, two users, and, a single GSO ground station. Fig. 4 presents the INR values over different placements of the GSO ground station at the equator over varying longitudes. For this simulation, it is assumed that the LEO satellite is located at coordinates (0, 25.6) and two LEO users at (-0.2, 25.6) and (0.2, 25.6), with the first value denoting the latitude and the second value indicating the longitude. When the GSO ground station and users are in close proximity, the interference rises for the scenarios with no interference mitigation, iCSI-BF and aCSI-BF. However, the proposed method effectively limits the interference in these events and assures a harmless interference level. It is important to highlight that the interference is already reduced by utilizing multi-beams, and beamforming techniques. Also, the drop of interference in the plot is due to the nulling point of the resulting antenna pattern. The impact of imperfect CSI on resulting INR levels is depicted in the zoomed-in plot. Later, we will observe that this effect becomes more pronounced with the increase of LEO users and the resulting accumulated differences. For the ZF method, we observe a significant reduction in interference, albeit at the expense of higher power consumption, which we will elaborate on later. Our proposed method restricts the maximum aggregate INR for the co-existing GSO terminals. We further evaluate the methods considering a broader scenario with multiple satellites and more number of users.

Fig. 5 presents the transmit power averaged over satellites for different values of users' SINR threshold. The beamforming power difference of our proposed method and ZF beamformer is substantial. The ZF method reduces interference to a greater extent, resulting in a considerable increase in the required power. Furthermore, we can observe that in beamforming power, the difference between considering AIC beamforming and not, is more evident when the users' SINR threshold increases. This means in order to meet the users' demand, higher power is required which translates into more emitted interfering power, necessitating greater beamforming power for mitigation. Moreover, the difference in beamforming power between using iCSI and aCSI is not significant. The power performance results for different interference thresholds at the GSO ground stations are plotted in Fig. 6. The results of iCSI-BF, aCSI-BF remain consistent due to the fact that these methods do not consider AIC and are not affected by the INR threshold value. Also, the ZF method does not consider the assigned threshold and nullifies the interference. The high power requirement of this benchmark is also apparent in this plot. For the proposed method we can see the power consumption will increase as the interference limit becomes stricter, i.e., a smaller INR threshold.

To further compare the methods, we illustrate the interference mitigation performance in Fig. 7. The plot is derived from the cumulative distribution function (CDF) of

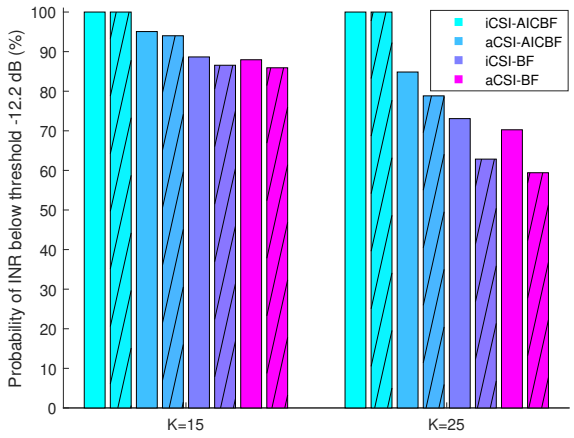

FIGURE 7. Probability percentage of interference levels below threshold, -12.2 dB at the GSO ground stations for different users per satellite. The plain bars present the results for $\gamma = 10$dB and the hatched ones show results for $\gamma = 12$dB.

the resulting INR values at each GSO location, iterated for random LEO users' positions. The percentage of times when the INR levels at restricted areas are less or equal to the INR threshold of -12.2dB is presented for two scenarios of different numbers of users. The results are presented for two different SINR thresholds for LEO users, where the plain bars demonstrate results for $\gamma = 10$dB, and the hatched ones are for $\gamma = 12$dB. To ensure clarity and readability, the results for the ZF method are not included in the plot. However, it's important to note that the INR compliance for all cases with iCSI-ZF and aCSI-ZF is 100%. Our proposed interference mitigation method proves to limit co-channel interference incidents when compared to the results of the no interference-constrained beamforming method where for the iCSI case the interference limitation is guaranteed 100%. As expected, our method provides less guarantee when considering aCSI instead of iCSI, however, it still shows a 95.07% interference avoidance performance for the case of 15 users and $\gamma = 10$dB.

Fig. 8 demonstrates the likelihood of meeting different interference thresholds at the GSO ground stations. Similarly, the results for the ZF method are omitted in this plot for clarity. However, it should be noted that the probability of limiting interference for the given threshold remains 100% for iCSI-ZF and aCSI-ZF with both user numbers scenarios. The probability of interference avoidance decreases as the thresholds get tighter. However, our proposed method with iCSI for both numbers of users guarantees perfect interference compliance. The proposed AIC beamforming with aCSI also demonstrates promising results for interference mitigation even at stricter interference thresholds.

Furthermore, the convergence behavior of Algorithm 1 is presented in Fig. 9 for a scenario with 10 users per satellite and 10 GSO ground stations, randomly located. Additionally, we set the parameters $\zeta = -14$ dB and $\gamma = 14$ dB in our

This article has been accepted for publication in IEEE Open Journal of the Communications Society. This is the author's version which has not been fully edited and content may change prior to final publication. Citation information: DOI 10.1109/OJCOMS.2024.3406530

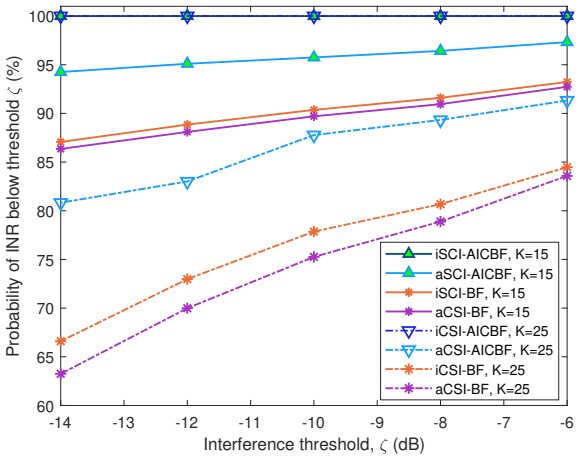

FIGURE 8. **Probability percentage of interference levels below threshold ζ at the GSO ground stations for different users per satellite with SINR threshold of $\gamma = 10$dB.**

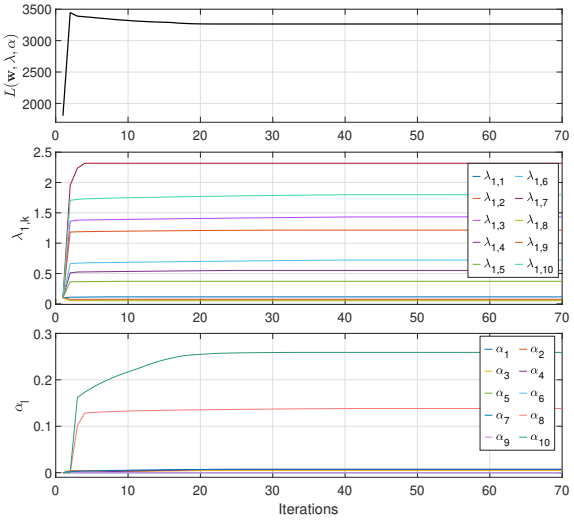

FIGURE 9. **Convergence plots of (from top to bottom): Lagrange function; Lagrangian multipliers $\lambda_{1,k=1:10}$; and Lagrangian multipliers $\alpha_{l=1:10}$**

simulation. The plots illustrate the convergence behavior of the Lagrangian function, as well as the Lagrangian multipliers $\lambda_{i,k}$ and α_l. For clarity purposes, we have plotted the values of the Lagrangian multiplier $\lambda_{i,k}$ for one satellite and its associated users. As we can see in the convergence plot for α_l multiplier, for some certain GSO ground station locations the INR constraint is already met, resulting in a final value of zero for the corresponding α_l. Moreover, as the plots illustrate the algorithm converges within a reasonable number of iterations.

B. GSO GROUND STATION LOCATION UNCERTAINTY RESULTS

In this subsection, we present the results of beamforming interference mitigation when the victims' locations are uncertain. The uncertainty level is considered as in equation (21) where we assume $a_x = a_y = 0$ and $b_x = b_y = b_{uc}$, and we calculate the results for the varying upper limit b_{uc}. Moreover, we consider these cases for deriving the results in this section as,

- **RAICBF**: We apply our robust AIC beamforming method summarized in Algorithm 2, where the beamformer is designed to satisfy users SINR and limit interference for GSO ground stations whose location information is uncertain and contains errors.
- **uc-AICBF**: For this case, we solve the beamforming problem using our previous AIC beamforming method defined in Algorithm 1. This is considered as a benchmark for evaluation.
- **BF**: presents the results where no interference mitigation method is applied and beamforming is applied to meet the users' SINR demands.

We calculate the results for the scenario with 15 users assuming users' SINR threshold of $\gamma = 10$dB, and interference threshold, $\zeta = -12.2$dB. Fig. 10 demonstrates the results for averaged satellite beamforming power over the error range of the arriving angle, applying the interference direction mismatch. We can see that the robust AIC beamformer requires more power in total, compared to the non-robust AIC beamformer. Moreover, the beamforming power exhibits only marginal increases for the presented error bounds. However, particularly at higher error levels, a greater increase in the power is observed. Despite the higher beamforming power requirement for RAICBF, the superior interference mitigation performance of the proposed robust method is evident in Fig. 11. This figure presents the probability of exceeding the interference limit at GSO ground stations for the uncertainty degrees. Our proposed RAICBF method has managed to control out-of-limit interference events even for the higher uncertainty levels. Nevertheless, with the uc-AICBF method, the interference probability decreases as the uncertainty bound increases. This is evident as with the increase of error in the GSO ground station location, the uc-AICBF method becomes less effective since it is not designed to mitigate the uncertainty and is vulnerable to the error in the positioning angles. In contrast, our proposed RAICBF overcomes this limitation by offering robustness against angular errors, thereby constraining interference at GSO receivers, maintaining a relatively stable probability despite the rising error bounds.

To conclude, as location error increases, RAICBF manages to prevent the exceeding interference events, but at the cost of higher transmission power. This creates a trade-off: uc-AICBF is sufficient for lower uncertainty degrees, while RAICBF provides better protection for the GSO ground stations, especially when experiencing high location uncertainty levels.

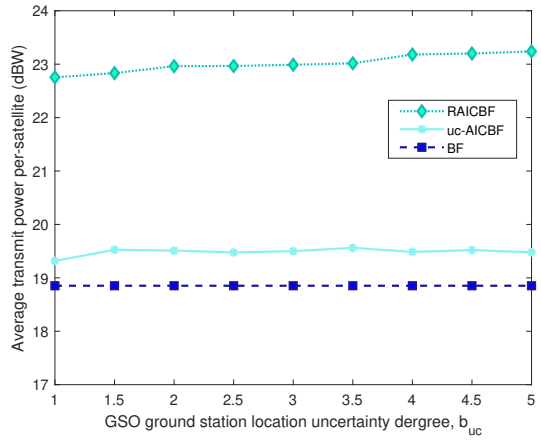

FIGURE 10. Mean satellite beamforming power for varying GSO ground stations uncertainty, assuming SINR threshold of $\gamma = 10$dB, $\zeta = -12.2$dB and $K = 15$ users.

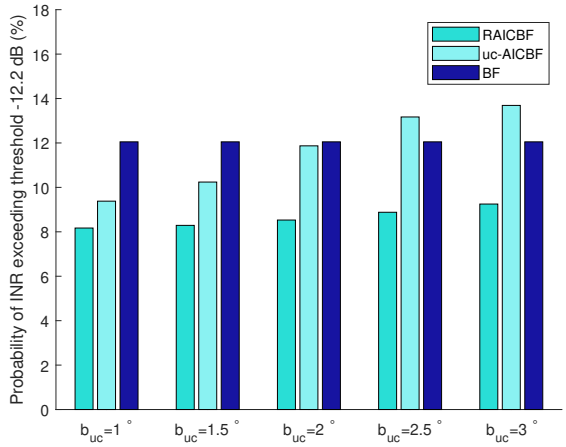

FIGURE 11. Probability percentage of interference levels above threshold ζ= -12.2dB at the GSO ground stations for different uncertainty levels, and LEO SINR threshold of $\gamma = 10$dB.

VI. CONCLUSION

This work considers interference compliance for NGSO satellites under AIC beamforming optimization, offering insights for enhancing satellite communication systems within the context of evolving LEO mega-constellations. Considering beamforming in multi-beam NGSO satellites reduces interference levels at GSO systems as presented by results, however, it falls short of complying with regulations. To address this, we proposed an AIC beamforming method ensuring limited aggregate interference levels at the GSO ground stations. The formulated problem was solved optimally, satisfying KKT conditions. Results demonstrate the efficacy of this method in managing the integrated interference at the co-existing GSO ground stations, compared with conventional beamforming methods. In addition to the imperfect CSI evaluated in our work, we have considered the uncertainty in GSO locations for the beamformer design. A robust AIC beamforming solution was developed to take account of the errors in the location-based CSI.

ACKNOWLEDGMENT

The authors would like to thank L. Emiliani from SES, Luxembourg, for providing valuable guidance on NGSO-to-GSO interference.

REFERENCES

[1] X. Lin, S. Cioni, G. Charbit, N. Chuberre, S. Hellsten, and J.-F. Boutillon, "On the path to 6G: Embracing the next wave of low earth orbit satellite access," *IEEE Communications Magazine*, vol. 59, no. 12, pp. 36–42, 2021.

[2] O. B. Osoro and E. J. Oughton, "A techno-economic framework for satellite networks applied to low earth orbit constellations: Assessing Starlink, OneWeb and Kuiper," *IEEE Access*, vol. 9, pp. 141 611–141 625, 2021.

[3] S. Liu, Z. Gao, Y. Wu, D. W. Kwan Ng, X. Gao, K.-K. Wong, S. Chatzinotas, and B. Ottersten, "LEO satellite constellations for 5G and beyond: How will they reshape vertical domains?" *IEEE Communications Magazine*, vol. 59, no. 7, pp. 30–36, 2021.

[4] O. Kodheli, E. Lagunas, N. Maturo, S. K. Sharma, B. Shankar, J. F. M. Montoya, J. C. M. Duncan, D. Spano, S. Chatzinotas, S. Kisseleff, J. Querol, L. Lei, T. X. Vu, and G. Goussetis, "Satellite communications in the new space era: A survey and future challenges," *IEEE Communications Surveys & Tutorials*, vol. 23, no. 1, pp. 70–109, 2021.

[5] Y. Su, Y. Liu, Y. Zhou, J. Yuan, H. Cao, and J. Shi, "Broadband LEO satellite communications: Architectures and key technologies," *IEEE Wireless Communications*, vol. 26, no. 2, pp. 55–61, 2019.

[6] H. Al-Hraishawi, H. Chougrani, S. Kisseleff, E. Lagunas, and S. Chatzinotas, "A survey on non-geostationary satellite systems: The communication perspective," *IEEE Communications Surveys & Tutorials*, 2022.

[7] C. Braun, A. M. Voicu, L. Simić, and P. Mähönen, "Should we worry about interference in emerging dense NGSO satellite constellations?" in *Proc. IEEE Int. Symp. Dyn. Spectr. Access Netw. (DySPAN)*, 2019, pp. 1–10.

[8] https://www.itu.int/hub/2023/10/key-issues-for-discussion-at-wrc%E2%80%9123/, [Online; accessed Jan. 2024].

[9] "Satellite transmission power battle drags on after WRC-23." [Online]. Available: https://spacenews.com/satellite-transmission-power-battle-drags-on-after-wrc-23/

[10] ITU-R, "Maximum permissible levels of interference in a satellite network (GSO/FSS; non-GSO/FSS; non-GSO/MSS feeder links) in the fixed-satellite service caused by other codirectional FSS networks below 30 GHz," *Recommendation S.1323-2*, 2002.

[11] M. Jalali, F. Ortiz-Gomez, F. Lagunas, S. Kisseleff, L. Emiliani, and S. Chatzinotas, " Radio Regulation Compliance of NGSO Constellations' Interference towards GSO Ground Stations," *IEEE International Symposium on Personal, Indoor and Mobile Radio Communications PIMRC*, 2022.

[12] ITU-R, "Methods to enhance sharing between non-GSO FSS systems (except MSS feeder links) in the frequency bands between 10-30 GHz," *Recommendation S.1431*, 2000.

[13] S. Tonkin and J. P. de Vries, "Newspace spectrum sharing: Assessing interference risk and mitigations for new satellite constellations,," *in Proc. TPRC, Washington, DC, USA*, 2018.

[14] M. Jalali, F. Ortiz, E. Lagunas, S. Kisseleff, L. Emiliani, and S. Chatzinotas, "Joint power and tilt control in satellite constellation for NGSO-GSO interference mitigation," *IEEE Open Journal of Vehicular Technology*, vol. 4, pp. 545–557, 2023.

[15] A. Hills, J. M. Peha, and J. Munk, "Feasibility of using beam steering to mitigate ku-band leo-to-geo interference," *IEEE Access*, vol. 10, pp. 74 023–74 032, 2022.

[16] https://www.starlink.com/technology, [Online; accessed Jan. 2024].

[17] T. Yoo and A. Goldsmith, "On the optimality of multiantenna broadcast scheduling using zero-forcing beamforming," *IEEE Journal on Selected Areas in Communications*, vol. 24, no. 3, pp. 528–541, 2006.

[18] J. Mitola and G. Maguire, "Cognitive radio: making software radios more personal," *IEEE Personal Communications*, vol. 6, no. 4, pp. 13–18, 1999.

[19] R. Saif, Z. Pourgharehkhan, S. ShahbazPanahi, M. Bavand, and G. Boudreau, "Underlay spectrum sharing in massive mimo systems," *IEEE Transactions on Cognitive Communications and Networking*, vol. 9, no. 3, pp. 647–663, 2023.

[20] X. Chen, H.-H. Chen, and W. Meng, "Cooperative communications for cognitive radio networks — from theory to applications," *IEEE Communications Surveys & Tutorials*, vol. 16, no. 3, pp. 1180–1192, 2014.

[21] Y. Noam and A. J. Goldsmith, "Blind null-space learning for mimo underlay cognitive radio with primary user interference adaptation," *IEEE Transactions on Wireless Communications*, vol. 12, no. 4, pp. 1722–1734, 2013.

[22] Y.-C. Liang, K.-C. Chen, G. Y. Li, and P. Mahonen, "Cognitive radio networking and communications: an overview," *IEEE Transactions on Vehicular Technology*, vol. 60, no. 7, pp. 3386–3407, 2011.

[23] S. Dadallage, C. Yi, and J. Cai, "Joint beamforming, power, and channel allocation in multiuser and multichannel underlay miso cognitive radio networks," *IEEE Transactions on Vehicular Technology*, vol. 65, no. 5, pp. 3349–3359, 2016.

[24] H. Du, T. Ratnarajah, M. Pesavento, and C. B. Papadias, "Joint transceiver beamforming in mimo cognitive radio network via second-order cone programming," *IEEE Transactions on Signal Processing*, vol. 60, no. 2, pp. 781–792, 2012.

[25] H. Islam, Y.-c. Liang, and A. T. Hoang, "Joint power control and beamforming for cognitive radio networks," *IEEE Transactions on Wireless Communications*, vol. 7, no. 7, pp. 2415–2419, 2008.

[26] L. Zhang, Y.-C. Liang, Y. Xin, and H. V. Poor, "Robust cognitive beamforming with partial channel state information," *IEEE Transactions on Wireless Communications*, vol. 8, no. 8, pp. 4143–4153, 2009.

[27] C.-G. Yang, J.-D. Li, and Z. Tian, "Optimal power control for cognitive radio networks under coupled interference constraints: A cooperative game-theoretic perspective," *IEEE Transactions on Vehicular Technology*, vol. 59, no. 4, pp. 1696–1706, 2010.

[28] G. Zheng, S. Ma, K.-k. Wong, and T.-S. Ng, "Robust beamforming in cognitive radio," *IEEE Transactions on Wireless Communications*, vol. 9, no. 2, pp. 570–576, 2010.

[29] D. Xu and Q. Li, "Joint power control and time allocation for wireless powered underlay cognitive radio networks," *IEEE Wireless Communications Letters*, vol. 6, no. 3, pp. 294–297, 2017.

[30] S. M. Almalfouh and G. L. Stüber, "Interference-aware radio resource allocation in ofdma-based cognitive radio networks," *IEEE Transactions on Vehicular Technology*, vol. 60, no. 4, pp. 1699–1713, 2011.

[31] E. Driouch and W. Ajib, "Downlink scheduling and resource allocation for cognitive radio mimo networks," *IEEE Transactions on Vehicular Technology*, vol. 62, no. 8, pp. 3875–3885, 2013.

[32] L. B. Le and E. Hossain, "Resource allocation for spectrum underlay in cognitive radio networks," *IEEE Transactions on Wireless Communications*, vol. 7, no. 12, pp. 5306–5315, 2008.

[33] L. Xu, H. Xing, Y. Deng, A. Nallanathan, and C. Zhuansun, "Fairness-aware throughput maximization for underlaying cognitive noma networks," *IEEE Systems Journal*, vol. 15, no. 2, pp. 1881–1892, 2021.

[34] P. Zuo, T. Peng, W. Linghu, and W. Wang, "Resource allocation for cognitive satellite communications downlink," *IEEE Access*, vol. 6, pp. 75 192–75 205, 2018.

[35] S. K. Sharma, S. Chatzinotas, and B. Ottersten, "Cognitive beamhopping for spectral coexistence of multibeam satellites," in *2013 Future Network & Mobile Summit*, 2013, pp. 1–10.

[36] C. Wang, D. Bian, S. Shi, J. Xu, and G. Zhang, "A novel cognitive satellite network with geo and leo broadband systems in the downlink case," *IEEE Access*, vol. 6, pp. 25 987–26 000, 2018.

[37] P. Angeletti and R. De Gaudenzi, "A Pragmatic Approach to Massive MIMO for Broadband Communication Satellites," *IEEE Access*, vol. 8, pp. 132 212–132 236, 2020.

[38] L. You, K.-X. Li, J. Wang, X. Gao, X.-G. Xia, and B. Ottersten, "Massive MIMO transmission for LEO satellite communications," *IEEE Journal on Selected Areas in Communications*, vol. 38, no. 8, pp. 1851–1865, 2020.

[39] K.-X. Li, L. You, J. Wang, X. Gao, C. G. Tsinos, S. Chatzinotas, and B. Ottersten, "Downlink transmit design for massive MIMO LEO satellite communications," *IEEE Transactions on Communications*, vol. 70, no. 2, pp. 1014–1028, 2022.

[40] T. Yue, A. Liu, and X. Liang, "Double-layer precoder and cluster-based power allocation design for LEO satellite communication with massive MIMO," *IEEE Communications Letters*, vol. 27, no. 2, pp. 650–654, 2023.

[41] E. Lagunas, A. Pérez-Neira, M. Martínez, M. A. Lagunas, M. A. Vázquez, and B. Ottersten, "Precoding with received-interference power control for multibeam satellite communication systems," *Frontiers in Space Technologies*, vol. 2, 2021. [Online]. Available: https://www.frontiersin.org/articles/10.3389/frspt.2021.662883

[42] M. Jalali, F. Ortiz, E. Lagunas, S. Kisseleff, S. Chatzinotas, and L. Emiliani, "LEO satellite beamforming for NGSO-GSO interference mitigation," *presented at the 40th International Communications Satellite Systems Conference (ICSSC)*, Oct. 2023.

[43] A.-A. Lu, X. Gao, W. Zhong, C. Xiao, and X. Meng, "Robust transmission for massive MIMO downlink with imperfect CSI," *IEEE Transactions on Communications*, vol. 67, no. 8, pp. 5362–5376, 2019.

[44] Y. Xu, X. Xia, K. Xu, and Y. Wang, "Three-dimension massive MIMO for air-to-ground transmission: Location-assisted precoding and impact of AoD uncertainty," *IEEE Access*, vol. 5, pp. 15 582–15 596, 2017.

[45] Y. Liu, Y. Wang, J. Wang, L. You, W. Wang, and X. Gao, "Robust downlink precoding for LEO satellite systems with per-antenna power constraints," *IEEE Transactions on Vehicular Technology*, vol. 71, no. 10, pp. 10 694–10 711, 2022.

[46] G. Zheng, K.-K. Wong, and B. Ottersten, "Robust cognitive beamforming with bounded channel uncertainties," *IEEE Transactions on Signal Processing*, vol. 57, no. 12, pp. 4871–4881, 2009.

[47] O. Raeesi, A. Gokceoglu, Y. Zou, E. Björnson, and M. Valkama, "Performance analysis of multi-user massive mimo downlink under channel non-reciprocity and imperfect csi," *IEEE Transactions on Communications*, vol. 66, no. 6, pp. 2456–2471, 2018.

[48] J. Wang, S. Han, S. Xu, and J. Li, "Snr-outage-based robust artificial noise-aided beamforming for correlated miso wiretap channels under gaussian channel uncertainties," *IEEE Systems Journal*, vol. 17, no. 1, pp. 1569–1580, 2023.

[49] Y. Chen, G. Zhang, H. Xu, Y. Ren, X. Chen, and R. Li, "Robust beamforming and power allocation for secure communication in systems with imperfect channel and hardware impairments," *IEEE Communications Letters*, vol. 26, no. 10, pp. 2277–2281, 2022.

[50] W. Yu and T. Lan, "Transmitter optimization for the multi-antenna downlink with per-antenna power constraints," *IEEE Transactions on Signal Processing*, vol. 55, no. 6, pp. 2646–2660, 2007.

[51] S. Maleki, S. Chatzinotas, B. Evans, K. Liolis, J. Grotz, A. Vanelli-Coralli, and N. Chuberre, "Cognitive spectrum utilization in Ka band multibeam satellite communications," *IEEE Communications Magazine*, vol. 53, no. 3, pp. 24–29, 2015.

[52] W. Tang, P. Thompson, and B. Evans, "Frequency sharing between satellite and terrestrial systems in the Ka band: A database approach," in *2015 IEEE International Conference on Communications (ICC)*, 2015, pp. 867–872.

[53] C. A. Balanis, *Antenna theory: analysis and design*. Wiley-Interscience, 2005.

[54] Y. Zhang, A. Liu, P. Li, and S. Jiang, "Deep learning (DL)-based channel prediction and hybrid beamforming for LEO satellite massive MIMO system," *IEEE Internet of Things Journal*, vol. 9, no. 23, pp. 23 705–23 715, 2022.

[55] T. Shi, Y. Liu, S. Kang, S. Sun, and R. Liu, "Angle-based multicast user selection and precoding for beam-hopping satellite systems," *IEEE Transactions on Broadcasting*, vol. 69, no. 4, pp. 856–871, 2023.

[56] A. Wiesel, Y. Eldar, and S. Shamai, "Linear precoding via conic optimization for fixed MIMO receivers," *IEEE Transactions on Signal Processing*, vol. 54, no. 1, pp. 161–176, 2006.

[57] L. Du, L. Li, H. Q. Ngo, T. C. Mai, and M. Matthaiou, "Cell-free massive MIMO: Joint maximum-ratio and zero-forcing precoder with power control," *IEEE Transactions on Communications*, vol. 69, no. 6, pp. 3741–3756, 2021.

[58] S. Boyd and L. Vandenberghe, *Convex Optimization*. Cambridge University Press, 2004.

[59] Z.-q. Luo, W.-k. Ma, A. M.-c. So, Y. Ye, and S. Zhang, "Semidefinite relaxation of quadratic optimization problems," *IEEE Signal Processing Magazine*, vol. 27, no. 3, pp. 20–34, 2010.

[60] K.-Y. Wang, A. M.-C. So, T.-H. Chang, W.-K. Ma, and C.-Y. Chi, "Outage constrained robust transmit optimization for multiuser MISO downlinks: Tractable approximations by conic optimization," *IEEE*

Transactions on Signal Processing, vol. 62, no. 21, pp. 5690–5705, 2014.
[61] ITU-R, "Apportionment of the allowable error performance degradations to fixed-satellite service (FSS) hypothetical Reference digital paths Srising from time invariant interference for systems operating below 30 GHz," *Recommendation S.1432-1*, 2006.
[62] E. Björnson and E. Jorswieck, 2013.
[63] ITU-R, "Satellite system characteristics to be considered in frequency sharing analyses between geostationary-satellite orbit (GSO) and non-GSO satellite systems in the fixed-satellite service (FSS) including feeder links for the mobile-satellite service (MSS)," *Recommendation S.1328-3*, 2002.
[64] ——, "Reference FSS earth-station radiation patterns for use in interference assessment involving non-GSO satellites in frequency bands between 10.7 GHz and 30 GHz," *Recommendation S.1428-1*, 2001.
[65] P. Gu, R. Li, C. Hua, and R. Tafazolli, "Dynamic Cooperative Spectrum Sharing in a Multi-Beam LEO-GEO Co-Existing Satellite System," *IEEE Transactions on Wireless Communications*, vol. 21, no. 2, pp. 1170–1182, 2022.

MAHDIS JALALI received her B.Sc. and M.Sc. degrees from the Department of Electrical Engineering at the Amirkabir University of Technology (Tehran Polytechnic), Iran. She is currently Ph.D. student at SIGCOM group in SnT, University of Luxembourg. Her research interests include satellite communication, resource management, and machine learning approaches for wireless communication systems.

EVA LAGUNAS received the M.Sc. and Ph.D. degrees in telecommunications engineering from the Polytechnic University of Catalonia (UPC), Barcelona, Spain, in 2010 and 2014, respectively. She was Research Assistant within the Department of Signal Theory and Communications, UPC, from 2009 to 2013. During the summer of 2009 she was a guest research assistant within the Department of Information Engineering, Pisa, Italy. From November 2011 to May 2012 she held a visiting research appointment at the Center for Advanced Communications (CAC), Villanova University, PA, USA. In 2014, she joined the Interdisciplinary Centre for Security, Reliability and Trust (SnT), University of Luxembourg, where she currently holds a Research Scientist position. Her research interests include terrestrial and satellite system optimization, spectrum sharing, resource management and machine learning.

ALIREZA HAQIQATNEJAD received the B.Sc. degree in electrical engineering from the Isfahan University of Technology, Isfahan, Iran, in 2012, the M.Sc. degree in telecommunications engineering from the University of Isfahan in 2015, and the Ph.D. degree in computer science from the Interdisciplinary Centre for Security, Reliability, and Trust (SnT), University of Luxembourg, Esch-sur-Alzette, Luxembourg, in 2021. He is currently a senior digital signal processing and telecommunications engineer at OQ Technology, Luxembourg. His current research/work involves signal processing and optimization for satellite communication systems, with a particular focus on 5G non-terrestrial networks and narrowband IoT.

STEVEN KISSELEFF (S'12, M'17, SM'22) received his M.Sc. degree in Information Technology from the Technical University of Kaiserslautern, Germany, and Ph.D. in Electrical Engineering from the Friedrich-Alexander University of Erlangen-Nürnberg (FAU), Germany in 2011 and 2017, respectively. From 2018 to 2023, he was with the SIGCOM Research Group at SnT, University of Luxembourg, at first as Research Associate and then as Research Scientist. In 2023, Dr. Kisseleff joined the Fraunhofer Institute for Integrated Circuits (IIS), Germany, where he currently holds a Senior Scientist position. His research interests include design and optimization of satellite networks, multi-antenna systems and internet of things.

SYMEON CHATZINOTAS (MEng, MSc, PhD, FIEEE) is currently Full Professor / Chief Scientist I and Head of the research group SIGCOM in the Interdisciplinary Centre for Security, Reliability and Trust, University of Luxembourg. In parallel, he is an Adjunct Professor in the Department of Electronic Systems, Norwegian University of Science and Technology and a Collaborating Scholar of the Institute of Informatics & Telecommunications, National Center for Scientific Research "Demokritos". In the past, he has lectured as Visiting Professor at the University of Parma, Italy and contributed in numerous R&D projects for the Institute of Telematics and Informatics, Center of Research and Technology Hellas and Mobile Communications Research Group, Center of Communication Systems Research, University of Surrey. He has received the M.Eng. in Telecommunications from Aristotle University of Thessaloniki, Greece and the M.Sc. and Ph.D. in Electronic Engineering from University of Surrey, UK in 2003, 2006 and 2009 respectively. He has authored more than 700 technical papers in refereed international journals, conferences and scientific books and has received numerous awards and recognitions, including the IEEE Fellowship and an IEEE Distinguished Contributions Award. He is currently in the editorial board of the IEEE Transactions on Communications, IEEE Open Journal of Vehicular Technology and the International Journal of Satellite Communications and Networking.